Proposed Coherent Trapping of a Population of Electrons in a C_{60} Molecule Induced by Laser Excitation

G. P. Zhang*
Department of Physics, Indiana State University, Terre Haute, Indiana 47809, USA

Thomas F. George
Office of the Chancellor and Center for Nanoscience, Departments of Chemistry & Biochemistry and Physics & Astronomy, University of Missouri-St. Louis, St. Louis, Missouri 63121, USA

(Received 22 June 2012; published 19 December 2012; corrected 3 June 2013)

This Letter demonstrates the possibility of generating coherent population trapping in C_{60}. Similar to a three-level Λ system, C_{60} has a forbidden transition between the highest occupied molecular orbital (HOMO) ($|a\rangle$) and the lowest unoccupied molecular orbital (LUMO) ($|c\rangle$), but a dipole-allowed transition between HOMO and LUMO + 1 ($|b\rangle$) and between $|b\rangle$ and $|c\rangle$. We employ two cw laser fields, one coupling and one probe. The strong coupling field is switched on first to resonantly excite the transition between $|b\rangle$ and $|c\rangle$. After a delay, the probe is switched on; the coherent interaction between the coupling and probe fields traps the population in $|a\rangle$ and $|c\rangle$. This forms a partially dark state in C_{60}, analogous to that in atomic vapors. Turning off the coupling field restores C_{60}'s absorption. Pulsed lasers work as well. We use two pulses to steer the system into a dark state; when we send in a cw probe field, the electric polarization of C_{60} plunges by five times, in comparison with the noncontrol case. This should be detectable experimentally.

DOI: 10.1103/PhysRevLett.109.257401 PACS numbers: 78.66.Tr, 42.50.Gy, 42.50.Md, 78.20.Bh

Coherent population trapping (CPT) [1–3] and electromagnetically induced transparency (EIT) [4] represent an important advancement in quantum optics and atomic physics, with broad applications from slowing [5] and stopping light [6,7], quantum memories [8], photon control in quantum information processing [9], storage of light [10,11] and information [12] to cancellation of Stark shifts in optical lattice clocks [13]. Very recently, EIT was extended to magnetically induced transparency in plasmas [14]. CPT and EIT are commonly observed in atomic vapors. They rely on two laser fields [1], one probe field E_1 and one coupling field E_2, to induce a coherent dark state for a medium which is inaccessible to the probe field, i.e., transparency. Those atoms feature a special energy scheme. Take a three-level Λ system as an example [see Fig. 1(a)]. Out of three possible transitions, only two are dipole allowed: one between states $|b\rangle$ and $|a\rangle$, and the other between states $|b\rangle$ and $|c\rangle$.

EIT is not exclusive to atomic systems [4]. In ruby, Zhao *et al.* [15] showed that it is possible to induce similar transparency via a magnetic field and a microwave field. Ichimura *et al.* [16], Beil *et al.* [17], Ham *et al.* [18], and Akhmedzhanov *et al.* [19] independently demonstrated similar effects in Pr-doped Y_2SiO_5 [11] and LaF_3 crystals. EIT can be induced in GaAs quantum wells [20] via biexciton coherence [21] or via electron spin coherence [22]. This was also observed in metallic nanoparticles [23]. In a solid, Longdell *et al.* showed that the storage time for the stopped light can be longer than one second [11]. The key to the success is that they were able to construct proper energy level schemes of either Λ, V or a cascade type [24]. Interestingly, these desirable energy level schemes are rather popular in fullerenes. Figure 1(a) shows a portion of the single-particle energy level scheme of C_{60} around the Fermi level, where H_u is the highest occupied molecular orbital, and T_{1u} and T_{1g} are the lowest and second lowest unoccupied molecular orbitals [25], respectively. For clarity, other energy levels are not shown. Just based on the symmetry argument, one immediately realizes that this system resembles a Λ system, a result that remains true even if we consider the many-body states [26].

As pointed out by Fleischhauer *et al.* [8], the application of EIT can be significantly broadened if it is implemented in a solid medium. One potential difficulty with solids is their shorter coherence time, but this is at least partially overcome in GaAs quantum wells via the intervalence band coherence effect [27]. We believe that going to nanostructured materials may strike a good balance between the applicability and the coherence time. Since these nanostructures can be engineered, they offer a larger flexibility and better chance for success. To the best of our knowledge, up to now, no investigation on fullerenes has ever been carried out either theoretically or experimentally. A theoretical investigation is very appropriate.

In this Letter, we show that C_{60} is an ideal system for coherent population trapping and electromagnetically induced transparency. We employ two cw laser fields to resonantly excite two dipole-allowed transitions, where one is from $|a\rangle$ to $|b\rangle$ and the other is from $|b\rangle$ to $|c\rangle$. We turn on the coupling laser first, and then after a delay,

 © 2012 American Physical Society

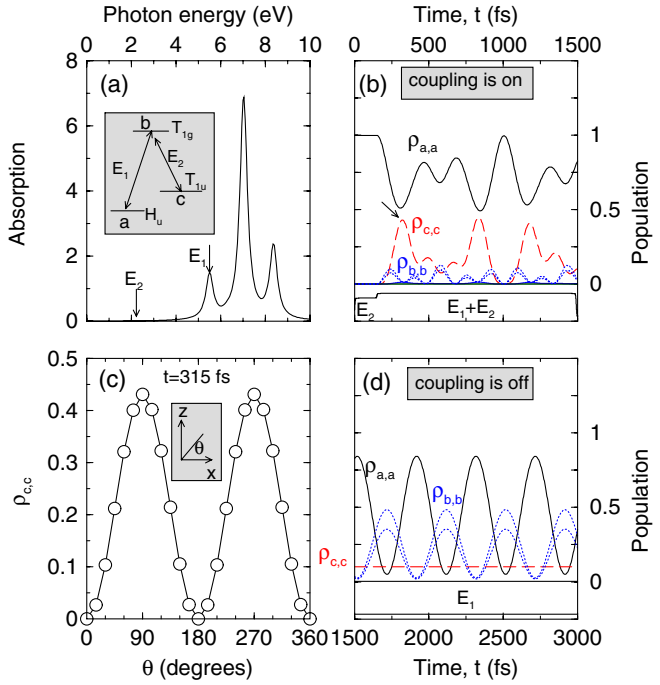

FIG. 1 (color online). (a) Absorption spectrum of C_{60}. The two arrows denote the excitation photon energies for the coupling and probe fields, respectively. The probe is E_1, and the coupling E_2. Inset: A typical Λ system, where the three levels $|a\rangle$, $|b\rangle$ and $|c\rangle$ refer to the ground state, one-photon-allowed and two-photon-allowed excited states. In the single-particle picture, these three levels correspond to the H_u, T_{1g}, and T_{1u} states, respectively. (b) Population change as a function of time with the coupling field on. The population is trapped between $|a\rangle$ and $|c\rangle$ by cw lasers. The solid line denotes ρ_{aa}, the long dashed line ρ_{cc}, and the two dotted lines refer to ρ_{bb}. The laser envelopes are shown at the bottom, where the coupling laser is turned on first and then the probe field. (c) Laser-polarization dependence of the population change in level $|c\rangle$ at time $t = 315$ fs. The coupling polarization changes from the x axis to the z axis, with the z axis along the fivefold symmetry axis. The inset shows the polarization angle. (d) Population change without the coupling field. Here the absorption is restored. The probe field envelope function is shown at the bottom.

we switch on the probe laser. We find the absorption of the probe by the system is reduced by a factor of 10, and the population is trapped in $|a\rangle$ and $|c\rangle$. When the coupling laser is off, the absorption is restored. Pulsed lasers allow more flexibility. We can purposely steer the population from the ground state $|a\rangle$ to the dipole-forbidden state $|c\rangle$ to form a partially dark state. In comparison with the noncoupling case, the polarization is reduced five times. These huge changes should be observable experimentally.

A typical Λ system consists of three special energy levels [see Fig. 1(a)]. In C_{60}, within a single particle picture, $|a\rangle$ may correspond to H_u, $|b\rangle$ to T_{1g}, and $|c\rangle$ to T_{1u}; other combinations of Λ or non-Λ systems are possible [28–30]. In the many-body picture, $|a\rangle$ corresponds to the ground state, $|b\rangle$ to the one-photon dipole-allowed state, and $|c\rangle$ to the two-photon dipole-allowed state, respectively, [see Fig. 1(a)]. All the excitation energies and transition matrix elements in this paper are computed within a single configuration interaction or CIS [31], with 200 excited states included in the configuration space to cover those low-lying dipole-allowed states [32]. Table I lists some of transition moments $\vec{\mu}_{ij}$ among these three states. Within these three states, the Hamiltonian can be written as [33]

$$H = \hbar\omega_a|a\rangle\langle a| + \hbar\omega_b|b\rangle\langle b| + \hbar\omega_c|c\rangle\langle c| - \mu_{ab}E_1|a\rangle\langle b| - \mu_{bc}E_2|b\rangle\langle c| + \text{H.c.}, \quad (1)$$

where $\hbar\omega_{a,b,c}$ are eigenenergies, and $E_{1(2)}$ is the probe (coupling) field. In C_{60}, these states are highly degenerate, but since there is no coupling among the degenerate states, they form respective subsets of Λ systems. The system evolves according to $|\Psi(t)\rangle = \sum_{\alpha=a,b,c} C_\alpha(t) \times \exp[-i\omega_\alpha t]|\alpha\rangle$, where C_α is the amplitude of each state. If both the fields are a continuum wave (cw) ($E_{1(2)}(t) = \frac{1}{2}(F_{1(2)}\exp[i\omega_{1(2)}t] + \text{H.c.}$), where F and ω are the amplitude and frequency, respectively), under the rotating wave approximation [34], C_α can be written analytically as

$$\dot{C}_a = -\frac{\mu_{ab}F_1}{2i\hbar}e^{i\Delta_1 t}C_b, \quad (2)$$

$$\dot{C}_b = -\frac{1}{2i\hbar}[\mu_{ba}F_1^* e^{-i\Delta_1 t}C_a + \mu_{bc}F_2^* e^{-i\Delta_2 t}C_c], \quad (3)$$

$$\dot{C}_c = -\frac{\mu_{cb}F_2}{2i\hbar}e^{i\Delta_2 t}C_b, \quad (4)$$

with $\Delta_1 = \omega_1 - (\omega_b - \omega_a)$ and $\Delta_2 = \omega_2 - (\omega_b - \omega_c)$. Coherent trapping relies on Eqs. (2) and (4). If we divide (2) by (4) and set $\Delta_1 = \Delta_2 = \Delta$, we obtain $\dot{C}_a\mu_{cb}F_2 - \dot{C}_c\mu_{ab}F_1 = 0$ or $C_c = \frac{\mu_{cb}F_2}{\mu_{ab}F_1}C_a + G$, where G is a constant determined by the initial condition. This is the essence of the coherent population trapping where the above equations permit a mixed state to trap populations between $|a\rangle$ and $|c\rangle$. Here, C_a and C_c have exactly the same time dependence. This is precisely what we find numerically in C_{60}.

We tune the probe to be resonant with the transition between the ground and one-photon states with $\hbar\omega_1 = 5.5025$ eV [see the first peak in the absorption spectrum in Fig. 1(a)]. The coupling field is resonant with the transition between the one- and two-photon states with $\hbar\omega_2 = 2.2194$ eV. The coupling field must be turned on first; otherwise, CPT is not effective (see Ref. [35]). Both fields are cw. To ramp up the field to a constant amplitude A_μ, we employ a steplike function

$$|\vec{F}_\mu(t)| = \frac{A_\mu}{\{1 + \exp[-2(t - T_\mu)/\tau_\mu]\}}\cos[\omega_\mu(t - T_\mu)], \quad (5)$$

TABLE I. Dipole transition moments (in atomic units) among the ground and excited states. Both $|b\rangle$ and $|c\rangle$ states are threefold degenerate, but only one state from $|c\rangle$ is listed.

	Ground state ($\|a\rangle$)			Excited state ($\|c\rangle$)		
Transition	$\langle a\|x\|b\rangle$	$\langle a\|y\|b\rangle$	$\langle a\|z\|b\rangle$	$\langle b\|x\|c\rangle$	$\langle b\|y\|c\rangle$	$\langle b\|z\|c\rangle$
Excited state ($\|b_1\rangle$)	−0.0416	1.5656	−1.1734	−0.5447	−0.0354	−0.0313
Excited state ($\|b_2\rangle$)	1.4884	0.7833	1.0028	−0.2673	0.4062	0.5497
Excited state ($\|b_3\rangle$)	1.2718	−0.8753	−1.2041	0.4648	0.2099	0.2665

where A_μ is the field amplitude, t is time, τ_μ is the ramp (for a Gaussian pulse, this refers to duration—see below), ω_μ is the laser center frequency, and T_μ is the time delay. This ramping avoids the numerical difficulty of dealing with a sharp step function. Our results are insensitive to the ramps, which are chosen to be $\tau = 4$ fs for both fields. After 200 laser periods of the probe field, or about 150 fs, the probe is switched on. The profiles of these two fields are shown in the bottom inset of Fig. 1(b). With both fields on, the population ρ is largely trapped in $|a\rangle$ (ρ_{aa}, solid black line) and $|c\rangle$ (ρ_{cc}, long dashed red line), with very little left in $|b\rangle$ (ρ_{bb}, dotted blue line). In other words, $|b\rangle$ becomes harder to excite; consequently, the system enters a partially dark state. Quantitatively, the average probabilities are 0.70, 0.05 and 0.25 for states $|a\rangle$, $|b\rangle$ and $|c\rangle$, respectively. We have made no attempt to completely deplete $|b\rangle$, or make the medium completely transparent, since ρ_{bb} is already so low, and the population is largely trapped between $|a\rangle$ and $|c\rangle$.

Since our numerical simulation includes all 200 excited states, we can check whether C_a and C_c indeed follow the prediction of the above Hamiltonian. Figure 1(b) shows clearly that C_a and C_c reach their respective extremes at nearly the same time, and the major physics is captured by the above model. However, there are some important differences between C_{60} and atomic systems. Because of the degeneracy of states, the populations in each state can take different amplitudes. For instance, the population in $|b\rangle$ has two dotted lines. This is because our current probe pulse is polarized along the x direction, where two degenerate states $|b_2\rangle$ and $|b_3\rangle$ have a strong dipole transition moment with the ground state (see Table I). Secondly, CPT strongly depends on the polarization of the fields. Figure 1(c) shows the polarization dependence of the population in state $|c\rangle$ at time $t = 315$ fs where the first peak of ρ_{cc} appears [see the arrow in Fig. 1(b)]. The polarization angle θ of the coupling field is measured from the x axis [see the inset in Fig. 1(c)]. When we rotate the coupling polarization from the x to z axis, ρ_{cc} increases sharply until $\theta = 90°$, but further rotation to the $-x$ axis diminishes the population. This change repeats every 180°. This means that the trapping is most effective when the polarizations of the coupling and probe fields are orthogonal to each other. The reason is that the orthogonal polarizations allow the coupling and probe to interact with the system independently, and there is no need to compete for the same excitation channel. This eventually leads to efficient population transfer. Although light polarization is hardly employed in atomic systems [8], it plays an important role in C_{60}.

Next we want to examine whether CPT is indeed induced by the coupling field. To do so, after 800 laser periods of E_2, we switch off the coupling field, and now the system evolves under influence of the probe alone. Figure 1(d) shows that the system immediately recovers its absorptive nature, with a huge oscillation in population between the ground state and excited state $|b\rangle$ [see the solid black line (ρ_{aa}) and two dotted blue lines (ρ_{bb}) in Fig. 1(d)]. The period of this oscillation can be found directly by solving Eqs. (2)–(4), except that here "$|b\rangle$" and "$|c\rangle$" should be interpreted as two degenerate states of $|b\rangle$, and F_2 is the same as F_1. Doing so, we find

$$C_a = Ae^{i\lambda_+ t/2} + Be^{i\lambda_- t/2} - \frac{\mu_{ab}\mu_{bc}F_1F_1^*}{\hbar^2\Omega^2}G, \quad (6)$$

where A and B are constants, the precession frequency of population is $\lambda_\pm = (\Delta \pm \sqrt{\Delta^2 + \Omega^2})$, and the generalized Rabi frequency is $\Omega = \sqrt{\Omega_1^2 + \Omega_2^2}$ with $\Omega_1^2 = |\mu_{ab}F_1|^2/\hbar^2$ and $\Omega_2^2 = |\mu_{bc}F_1|^2/\hbar^2$. With $\Delta = 0$, the frequency is just Ω. Using our current parameters, we find the theoretical period is 399.43 fs, which matches extremely well with our numerical result of 400.6 fs. This validates again the above three-level model as describing C_{60} well.

CPT is not exclusive to the continuum wave. Pulsed lasers give us additional new degrees of freedom to control the dynamics. We first employ two Gaussian pulses,

$$|\vec{E}_\mu(t)| = A_\mu \exp[-(t - T_\mu)^2/\tau_\mu^2]\cos[\omega_\mu(t - T_\mu)], \quad (7)$$

to prepare the system in a partially dark state. One short pulse, with duration $\tau_1 = 12$ fs, $A_1 = 0.1$ V/Å and photon energy $\hbar\omega_1 = 5.5$ eV, is fired at 0 fs to resonantly excite the transition from the ground state $|a\rangle$ to the dipole-allowed state $|b\rangle$. Figure 2(a) shows that under the influence of the laser pulse, $|a\rangle$ loses population to $|b\rangle$. Two sublevels of the threefold degenerate $|b\rangle$ state have substantial populations [see $\rho_{b1,b1}$ and $\rho_{b2,b2}$ in Fig. 2(a)]. We delay the second pulse to $T_2 = 100$ fs, which is necessary since it gives the first pulse enough time to fully populate the $|b\rangle$ state. Similar to the first pulse, we resonantly excite transitions between $|c\rangle$ and $|b\rangle$ with photon energy of

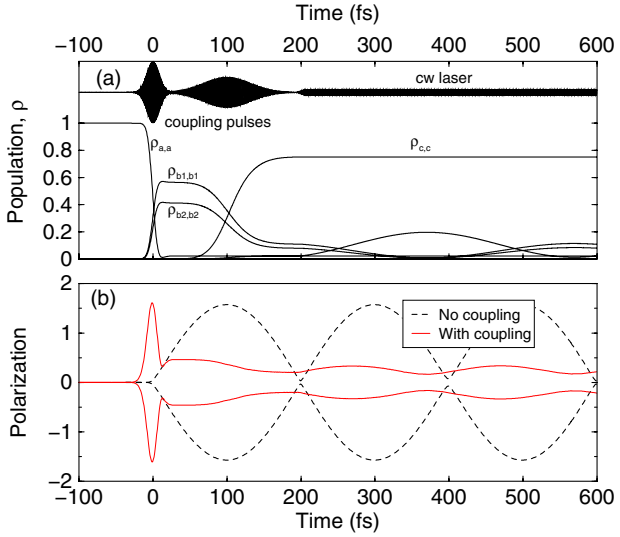

FIG. 2 (color online). (a) CPT induced by the pulse laser fields. Two coupling pulses prepare the system in a dark state. When the cw probe field enters, it becomes much less absorptive. The laser fields are shown at the top. (b) Envelopes of polarization with (solid red line) and without (long dashed line) the coupling pulses. The change in polarization differs by five times.

$\hbar\omega_2 = 2.2194$ eV. Figure 2(a) shows that after 100 fs, $|b\rangle$ suffers a big loss in its population, while ρ_{cc} gains substantially. After 200 fs, when both pulses have gone, the system is partially in a transparent state.

To test the transparency, we fire a cw probe around 200 fs, and find the amplitude of the population oscillation is only about 0.2 [see Fig. 2(a)]. Such a reduction can be clearly seen in the polarization $P = \mathrm{Tr}(\rho D)$. Figure 2(b) shows the polarization envelopes for two cases: one without coupling pulses (long dashed black line), and the other with coupling pulses (solid red line). Under normal cw excitation, P oscillates very strongly (long dashed black line). But when the system is prepared in the dark state, such an oscillation in P is reduced five times, from 1.50 to 0.30 (same arbitrary units). We expect such a transient polarization can be probed experimentally [36–38].

In conclusion, we have demonstrated coherent population trapping in C_{60}. CPT can be induced by a cw laser or pulsed laser. In the cw excitation, the coupling field impinges the system ahead of the probe field. Whenever the coupling field is on, the population in the one-photon-dipole-allowed state $|b\rangle$ is very small, the system enters a dark state, and the absorption is substantially weakened. However, if the coupling field is off, the system becomes absorptive again. Using pulsed lasers, one can trap the population in states $|a\rangle$ and $|c\rangle$ and deplete state $|b\rangle$, or partial transparency to the probe field. The electric polarization is decreased by five times. It is of great interest to test our predictions experimentally.

This work was supported by the U.S. Department of Energy under Contract No. DE-FG02-06ER46304. Part of the work was done on Indiana State University's high-performance computers. This research used resources of the National Energy Research Scientific Computing Center, which is supported by the Office of Science of the U.S. Department of Energy under Contract No. DE-AC02-05CH11231. Our calculations also used resources of the Argonne Leadership Computing Facility at Argonne National Laboratory, which is supported by the Office of Science of the U.S. Department of Energy under Contract No. DE-AC02-06CH11357.

*gpzhang@indstate.edu

[1] H. R. Gray, R. M. Whitley, and C. R. Stroud, Opt. Lett. **3**, 218 (1978); E. Arimondo, in *Progress in Optics,* edited by E. Wolf (Elsevier, Amsterdam, 1996), Vol. 35, p. 257.
[2] M. O. Scully and M. S. Zubairy, *Quantum Optics* (Cambridge University Press, Cambridge, England, 2006).
[3] X. Xu, B. Sun, P. R. Berman, D. G. Steel, A. S. Bracker, D. Gammon, and L. J. Sham, Nat. Phys. **4**, 692 (2008).
[4] S. E. Harris, Phys. Today **50**, 36 (1997); K. J. Boller, A. Imamoglu, and S. E. Harris, Phys. Rev. Lett. **66**, 2593 (1991).
[5] L. V. Hau, S. E. Harris, Z. Dutton, and C. H. Behroozi, Nature (London) **397**, 594 (1999).
[6] Z. Dutton, N. S. Ginsberg, C. Slowe, and L. V. Hau, Europhysics News **35**, 33 (2004).
[7] A. V. Turukhin, V. S. Sudarshanam, M. S. Shahriar, J. A. Musser, B. S. Ham, and P. R. Hemmer, Phys. Rev. Lett. **88**, 023602 (2001).
[8] M. Fleischhauer, A. Imamoglu, and J. P. Marangos, Rev. Mod. Phys. **77**, 633 (2005).
[9] M. D. Lukin and A. Imamoglu, Nature (London) **413**, 273 (2001).
[10] D. F. Phillips, A. Fleischhauer, A. Mair, R. L. Walsworth, and M. D. Lukin, Phys. Rev. Lett. **86**, 783 (2001).
[11] J. J. Longdell, E. Fraval, M. J. Sellars, and N. B. Manson, Phys. Rev. Lett. **95**, 063601 (2005).
[12] C. Liu, Z. Dutton, C. H. Behroozi, and L. V. Hau, Nature (London) **409**, 490 (2001).
[13] T. Zanon-Willette, A. D. Ludlow, S. Blatt, M. M. Boyd, E. Arimondo, and J. Ye, Phys. Rev. Lett. **97**, 233001 (2006).
[14] R. Gad, J. G. Leopold, A. Fisher, D. R. Fredkin, and A. Ron, Phys. Rev. Lett. **108**, 155003 (2012).
[15] Y. Zhao, C. Wu, B. S. Ham, M. K. Kim, and E. Awad, Phys. Rev. Lett. **79**, 641 (1997).
[16] K. Ichimura, K. Yamamoto, and N. Gemma, Phys. Rev. A **58**, 4116 (1998).
[17] F. Beil, J. Klein, G. Nikoghosyan, and T. Halfmann, J. Phys. B **41**, 074001 (2008).
[18] B. S. Ham, M. S. Shahriar, M. K. Kim, and P. R. Hemmer, Opt. Lett. **22**, 1849 (1997).
[19] R. A. Akhmedzhanov, A. A. Bondartsev, L. A. Gushchin, and I. V. Zelensky, JETP Lett. **94**, 544 (2011).
[20] G. B. Serapiglia, E. Paspalakis, C. Sirtori, K. L. Vodopyanov, and C. C. Phillips, Phys. Rev. Lett. **84**, 1019 (2000).
[21] M. C. Phillips, H. Wang, I. Rumyantsev, N. H. Kwong, R. Takayama, and R. Binder, Phys. Rev. Lett. **91**, 183602 (2003).

[22] H. Wang and S. O'Leary, J. Opt. Soc. Am. B **29**, A6 (2012).
[23] V. Yannopapas, E. Paspalakis, and N. V. Vitanov, Phys. Rev. B **80**, 035104 (2009).
[24] M. Lindberg and R. Binder, Phys. Rev. Lett. **75**, 1403 (1995).
[25] J. O. Johansson, G. G. Henderson, F. Remacle, and E. E. B. Campbell, Phys. Rev. Lett. **108**, 173401 (2012).
[26] G. P. Zhang, D. A. Strubbe, S. G. Louie, and T. F. George, Phys. Rev. A **84**, 023837 (2011).
[27] M. C. Phillips and H. Wang, Opt. Lett. **28**, 831 (2003).
[28] G. P. Zhang, Phys. Rev. Lett. **91**, 176801 (2003).
[29] G. P. Zhang and T. F. George, Phys. Rev. Lett. **93**, 147401 (2004).
[30] G. P. Zhang, Phys. Rev. Lett. **95**, 047401 (2005).
[31] M. J. Frisch *et al.*, *GAUSSIAN03*, (Gaussian Inc., Pittsburgh, PA, 2003).
[32] Our theoretical absorption spectrum at CIS level is only qualitatively consistent with the experimental spectrum [Y. Wang, J. M. Holden, A. M. Rao, W.-T. Lee, X. X. Bi, S. L. Ren, G. W. Lehman, G. T. Hager, and P. C. Eklund, Phys. Rev. B **45**, 14 396 (1992)], but the peak at 5.5 eV almost exactly matches the experimental peak. While GAUSSIAN03 allows the inclusion of additional electron correlation effects through EOM-CCSD to get a better linear absorption spectrum, it does not provide the transition matrix elements among excited states. However, our result in the Letter is independent of the limitation of GAUSSIAN03. In our prior tight-binding approach [G. P. Zhang, X. Sun, and T. F. George, Phys. Rev. B **68**, 165410 (2003)], our absorption spectrum is closer to the experimental one, though the correlation effect is missed.
[33] The conditions under which the analytical solutions could be obtained are when (a) the system can be approximated by three levels, (b) the degeneracy in each energy level can be ignored, and (c) the light polarization can be ignored.
[34] G. P. Zhang, Phys. Rev. Lett. **101**, 187203 (2008).
[35] J. R. Kuklinski, U. Gaubatz, F. T. Hioe, and K. Bergmann, Phys. Rev. A **40**, 6741 (1989).
[36] Y. Li and M. Xiao, Opt. Lett. **20**, 1489 (1995).
[37] H. X. Chen, A. V. Durrant, J. P. Marangos, and J. A. Vaccaro, Phys. Rev. A **58**, 1545 (1998).
[38] S. Marcinkevicius, A. Gushterov, and J. P. Reithmaier, Appl. Phys. Lett. **92**, 041113 (2008).